

Building and evaluation of a PBPK model for Ethinylestradiol in adults

Version	1.1-OSP10.0
based on <i>Model Snapshot</i> and <i>Evaluation Plan</i>	https://github.com/Open-Systems-Pharmacology/Ethinylestradiol-Model/releases/tag/v1.0
OSP Version	10.0
Qualification Framework Version	2.3

This evaluation report and the corresponding PK-Sim project file are filed at:

<https://github.com/Open-Systems-Pharmacology/OSP-PBPK-Model-Library/>

Table of Contents

- [1 Introduction](#)
- [2 Methods](#)
 - [2.1 Modeling Strategy](#)
 - [2.2 Data](#)
 - [2.3 Model Parameters and Assumptions](#)
- [3 Results and Discussion](#)
 - [3.1 Final input parameters](#)
 - [3.2 Diagnostics Plots](#)
 - [3.3 Concentration-Time Profiles](#)
 - [3.3.1 Model Building](#)
 - [3.3.2 Model Verification](#)
- [4 Conclusion](#)
- [5 References](#)
- [6 Glossary](#)

1 Introduction

The presented PBPK model of ethinylestradiol (EE) has been developed to be used in a PBPK Drug-Drug-Interactions (DDI) network with ethinylestradiol as perpetrator of CYP1A2.

Ethinylestradiol is an estrogen medication which is used widely as a birth control pills in combination with progestins. The following ADME properties characterize ethinylestradiol ([SmPC Namuscla](#), [FDA QUARTETTE](#)):

Absorption: ethinylestradiol is rapidly and completely absorbed from the gut but it undergoes some first pass metabolism in the gut wall (mediated by a.o. CYP3A4 ([Wiesinger 2015](#), [Wang 2004](#))). After oral administration, an initial peak occurs in plasma at 2 to 3 hours, with a secondary peak at about 12 hours after dosing; the second peak is interpreted as evidence for extensive enterohepatic circulation of ethinylestradiol.

Distribution: ethinylestradiol is rapidly distributed throughout most body tissues with the largest concentration found in adipose tissue. It distributes into breast milk, with low concentrations. More than 80% of ethinylestradiol in serum is conjugated as sulphate and almost all the conjugated form is bound to albumin.

Metabolism: ethinylestradiol is metabolised in the liver. Hydroxylation appears to be the main metabolic pathway. 60% of a dose is excreted in the urine and 40% in the faeces.

Excretion: About 30% is excreted in the urine and bile as the glucuronide or sulphate conjugate. The rate of metabolism of ethinylestradiol is affected by several factors, including enzyme-inducing agents, antibiotics, and cigarette smoking. The elimination half-life of ethinylestradiol ranges from 5 to 16 hours.

After i.v administration, ethinylestradiol displays approximately linear dose relationship in the dose range 30-100 µg. A wide variability is present in the terminal part of the dose-normalized concentrations.

After p.o. single dose, ethinylestradiol shows linear dose relationship in the dose range 30-3000 µg. Secondary peaks can be observed in individual data, compatible with enterohepatic re-circulation. However, mean data do not display such feature as a result of such peak being averaged out. Therefore, enterohepatic re-circulation was not taken into account in the model.

2 Methods

2.1 Modeling Strategy

The general workflow for building an adult PBPK model has been described by Kuepfer et al. ([Kuepfer 2016](#)). Relevant information on the anthropometry (height, weight) was gathered from the respective clinical study, if reported. Information on physiological parameters (e.g. blood flows, organ volumes, hematocrit) in adults was gathered from the literature and has been incorporated in PK-Sim® as described previously ([Willmann 2007](#)). The applied activity and variability of plasma proteins and active processes that are integrated into PK-Sim® are described in the publicly available 'PK-Sim® Ontogeny Database Version 7.3' ([PK-Sim Ontogeny Database Version 7.3](#)).

The following steps were undertaken in model development:

1. Define lipophilicity and distribution model on data after i.v. administration with linear total hepatic clearance fitted to data and renal clearance set to literature value ([Ezuruike 2018](#)).
2. Predict p.o. data after single dose and at steady state
3. Detail metabolic contribution of different CYPs and UGTs to total hepatic clearance.

Details about input data (physicochemical, *in vitro* and clinical) can be found in [Section 2.2](#).

Details about the structural model and its parameters can be found in [Section 2.3](#).

A standard female subject was created based on the European (ICRP,2002) PK-Sim database (age = 30 y, weight = 60 kg, height = 163 cm, BMI = 22,58 kg/m²) and used for simulations, until stated otherwise. Expression of the enzymes CYP3A4, CYP2C9, CYP1A2, CYP2C8, and UGT1A1 from RT PCR database were added.

2.2 Data

2.2.1 In vitro and physico-chemical data

A literature search was performed to collect available information on physico-chemical properties of ethinylestradiol ([Table 1](#)).

Parameter	Unit	Value	Source	Description
MW ⁺	g/mol	296.4	DrugBank DB00977	Molecular weight
pK _{a,acid} ⁺		10.33	DrugBank DB00977	Acidic dissociation constant
Solubility (pH) ⁺	mg/mL	6.77e-3 (7)	DrugBank DB00977	Aqueous Solubility
logD		3.63 - 3.9	DrugBank DB00977	Distribution coefficient
fu ⁺	%	3	DrugBank DB00977	Fraction unbound in plasma
CYP1A2 CL ⁺	μl/min/pmol	0.51	Ezuruike 2018	Clearance by CYP1A2
CYP2C8 CL ⁺	μl/min/pmol	0.13	Ezuruike 2018	Clearance by CYP2C8
CYP2C9 CL ⁺	μl/min/pmol	0.51	Ezuruike 2018	Clearance by CYP2C9
CYP3A4 CL ⁺	μl/min/pmol	0.5	Ezuruike 2018	Clearance by CYP3A4
K _m UGT1A1 ⁺	μmol/l	19.22	Ezuruike 2018	UGT1A1 saturation constant
V _{max} UGT1A1 ⁺	pmol/min/mg prot.	408.5	Ezuruike 2018	Maximal metabolization rate by UGT1A1
Renal Elimination ⁺	l/h	2.079	Stanczyk 2013	Renal clearance
Cl _{int} HLM ⁺	μL/min/mg prot.	118.83	Ezuruike 2018	Intrinsic clearance in Human Liver Microsomes
K _i CYP1A2	μmol/l	10.6	Karjalainen 2008	CYP1A2 inhibition constant

Table 1: Physico-chemical and *in-vitro* metabolization properties of ethinylestradiol extracted from literature. ⁺: Value used in final model

2.2.2 Clinical data

A literature search was performed to collect available clinical data on ethinylestradiol ([Table 2](#)).

Source	Route	Dose [mg]/ Schedule *	Pop.	Sex	N	Form.
Back 1981 ⁺	i.v.	0.03	HV	F	5	solution
Back 1981 ⁺	p.o.	0.03	HV	F	5	tablet
Back 1979 ⁺	i.v.	0.05	HV	F	6	solution
Back 1979 ⁺	p.o.	0.05	HV	F	6	NA
Back 1987	p.o.	0.05 q.d.	HV	F	5	tablet
Orme 1991 ⁺	i.v.	0.03	HV	F	10	solution
Orme 1991 ⁺	p.o.	0.03	HV	F	10	tablet
Kuhnz 1996	i.v.	0.06	HV	F	19	solution
Goebelsmann 1986 ⁺	p.o.	0.03	HV	F	24	solution and tablet
Stanczyk 1983 ⁺	p.o.	0.12	HV	F	24	solution and tablet
Zhang 2017 ⁺	p.o.	0.03	HV	F	12	tablet
Martin 2016	p.o.	0.03 q.d.	HV	F	27	tablet
Stockis 2014	p.o.	0.03 q.d.	HV	F	24	tablet
Sidhu 2006	p.o.	0.03 q.d.	HV	F	16	tablet
Kothare 2012 ⁺	p.o.	0.03/0.03 q.d.	HV	F	20	tablet
Timmer 2000 ⁺	p.o.	0.03	HV	F	-	tablet

Table 2: Literature sources of clinical concentration data of ethinylestradiol used for model development and validation. *: *single dose unless otherwise specified*; ⁺: *Data used for final parameter identification*

2.3 Model Parameters and Assumptions

2.3.1 Absorption

Intestinal permeability was fitted to po data. Formulation of ethinylestradiol tablet was modeled with Weibull-function and parameters **Dissolution time (50% dissolved)** and **Lag time** fitted to po data.

2.3.2 Distribution

Physico-chemical parameters were set to the reported values (see [Section 2.2.1](#)). It was assumed that the major binding partner in plasma is albumin. The value of lipophilicity was estimated by fitting the model to iv and po data.

After testing the available organ-plasma partition coefficient and cell permeability calculation methods available in PK-Sim, observed clinical data were best described by choosing the partition coefficient calculation by **Berezhkovskiy** and cellular permeability calculation by **PK-Sim Standard**.

2.3.3 Metabolism and Elimination

Following metabolization processes have been implemented based on [Ezuruike 2018](#):

- Linear CYP1A2 CL
- Linear CYP2C8 CL
- Linear CYP2C9 CL
- Linear CYP3A4 CL
- Saturable UGT1A1
- Unspecific liver metabolization

Renal plasma clearance is modeled with `Plasma cLeaRance` set to 2.079 l/h reported in literature ([Stanczyk 2013](#)). The value was normalized to body weight by dividing by 70 kg.

2.3.4 Enzyme Inhibition

Simulations of co-administration of ethinylestradiol with tizanidine (see [CYP1A2 DDI Qualification report](#)) indicate that the reported competitive inhibition of CYP1A2 by ethinylestradiol ([Karjalainen 2008](#)) is not sufficient to describe the increased concentrations of tizanidine after multiple days administration. Therefore, it was decided to fit a time-dependent inhibition (TDI) function to the CYP1A2 enzyme system. The parameters `kinact` and `K_kinact_half` were estimated by fitting the model to concentration-time profiles of tizanidine ([Granfors 2005](#)).

2.3.5 Automated Parameter Identification

Following parameter values were estimated for the model:

- `Lipophilicity`
- `Specific intestinal permeability`
- `Dissolution time (50% dissolved)` (Weibull formulation)
- `Lag time` (Weibull formulation)
- `kinact` (CYP1A2 TDI)
- `K_kinact_half` (CYP1A2 TDI)

3 Results and Discussion

The next sections show:

1. Final model input parameters for the building blocks: [Section 3.1](#).
2. Overall goodness of fit: [Section 3.2](#).
3. Simulated vs. observed concentration-time profiles for the clinical studies used for model building and for model verification: [Section 3.3](#).

3.1 Final input parameters

The parameter values of the final PBPK model are illustrated below.

Formulation: Ethinylestradiol tablet

Type: Weibull

Parameters

Name	Value	Value Origin
Dissolution time (50% dissolved)	36.5087007601 min	Parameter Identification
Lag time	6.7747764588 min	Parameter Identification
Dissolution shape	0.92	
Use as suspension	Yes	

Compound: Ethinylestradiol

Parameters

Name	Value	Value Origin	Alternative	Default
Solubility at reference pH	0.00677 mg/ml	Database-DrugBank DB00977	S_aq	True
Reference pH	7	Database-DrugBank DB00977	S_aq	True
Lipophilicity	3.4805414593 Log Units	Parameter Identification	LogP	True
Fraction unbound (plasma, reference value)	0.03	Database-DrugBank DB00977	fu_plasma	True
Specific intestinal permeability (transcellular)	0.000168 cm/min	Parameter Identification	Fit	True
Is small molecule	Yes			
Molecular weight	296.4 g/mol	Database-DrugBank DB00977		
Plasma protein binding partner	Albumin			

Calculation methods

Name	Value
Partition coefficients	Berezhkovskiy
Cellular permeabilities	PK-Sim Standard

Processes

Metabolizing Enzyme: CYP1A2-Ezuruike_2018

Molecule: CYP1A2

Parameters

Name	Value	Value Origin
In vitro CL/recombinant enzyme	0.51 µl/min/pmol rec. enzyme	Publication-Ezuruike 2018

Metabolizing Enzyme: CYP2C8-Ezuruike_2018

Molecule: CYP2C8

Parameters

Name	Value	Value Origin
In vitro CL/recombinant enzyme	0.13 µl/min/pmol rec. enzyme	Publication-Ezuruike 2018

Metabolizing Enzyme: CYP2C9-Ezuruike_2018

Molecule: CYP2C9

Parameters

Name	Value	Value Origin
In vitro CL/recombinant enzyme	0.51 µl/min/pmol rec. enzyme	Publication-Ezuruike 2018

Metabolizing Enzyme: CYP3A4-Ezuruike_2018

Molecule: CYP3A4

Parameters

Name	Value	Value Origin
In vitro CL/recombinant enzyme	0.5 µl/min/pmol rec. enzyme	Publication-Ezuruike 2018

Metabolizing Enzyme: UGT1A1-Ezuruike_2018

Molecule: UGT1A1

Parameters

Name	Value	Value Origin
In vitro Vmax for liver microsomes	408.5 pmol/min/mg mic. protein	Publication-Ezuruike 2018
Content of CYP proteins in liver microsomes	33.6 pmol/mg mic. protein	Publication-Ezuruike 2018
Km	19.22 $\mu\text{mol/l}$	Publication-Ezuruike 2018

Systemic Process: Renal Clearances-Stanczyk_2013

Species: Human

Parameters

Name	Value	Value Origin
Fraction unbound (experiment)	0.03	
Plasma clearance	0.0285 l/h/kg	Publication-Stanczyk_2013; $2.079/73=$

Systemic Process: Total Hepatic Clearance-Ezuruike_2018

Species: Human

Parameters

Name	Value	Value Origin
Fraction unbound (experiment)	0.03	
Lipophilicity (experiment)	3.4805414593 Log Units	
Plasma clearance	0 ml/min/kg	
Specific clearance	1.1002777778 1/min	Publication-Ezuruike 2018 - Calculated from 118.83 $\mu\text{l/min/mg mic. protein}$ divided by 108 pmol/mg/ mic. protein

Inhibition: CYP1A2-Fit

Molecule: CYP1A2

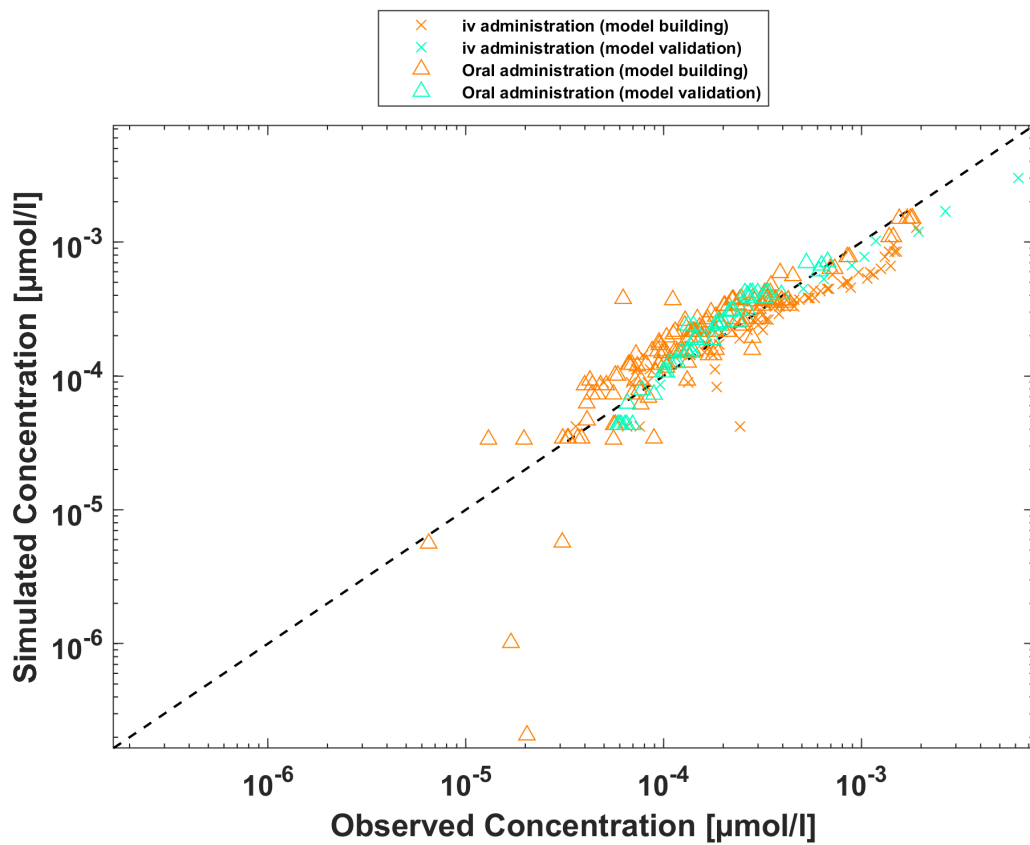
Parameters

Name	Value	Value Origin
kinact	200 1/min	Parameter Identification
K_kinact_half	0.4833013314 $\mu\text{mol/l}$	Parameter Identification

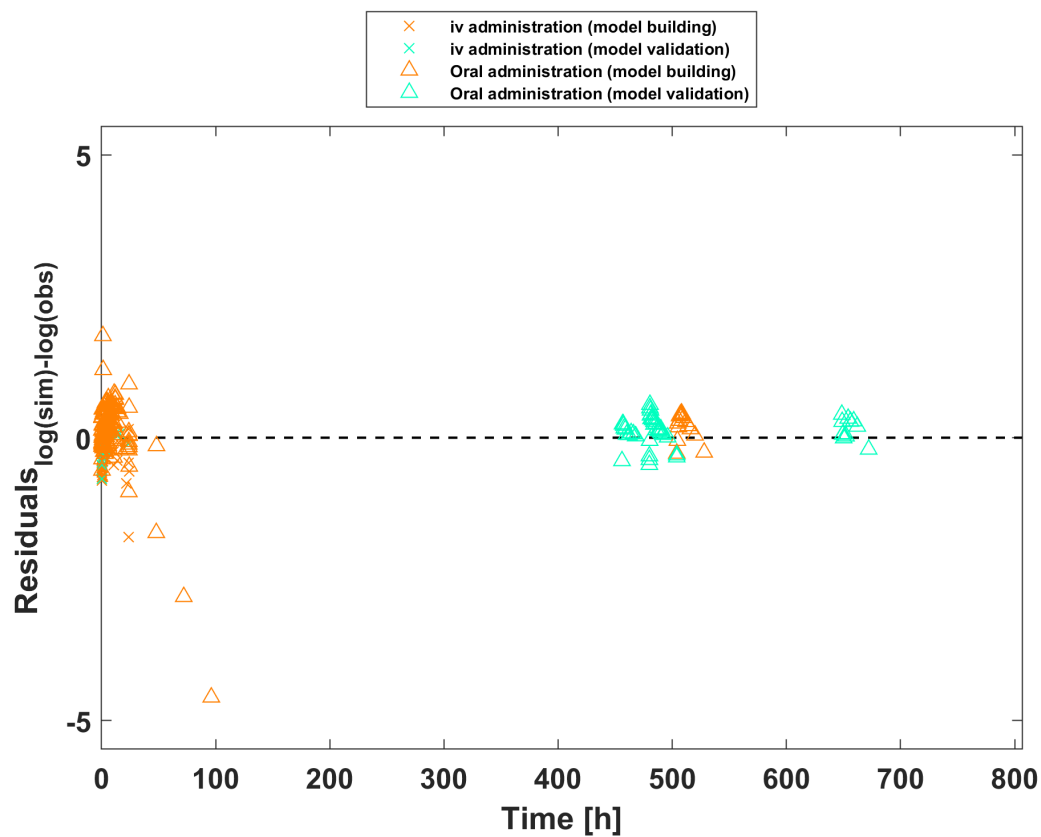
3.2 Diagnostics Plots

The following section displays the goodness-of-fit visual diagnostic plots for the PBPK model performance of all data listed in [Section 2.2.2](#).

The first plot shows observed versus simulated plasma concentration, the second weighted residuals versus time.



Ethinylestradiol concentration in plasma



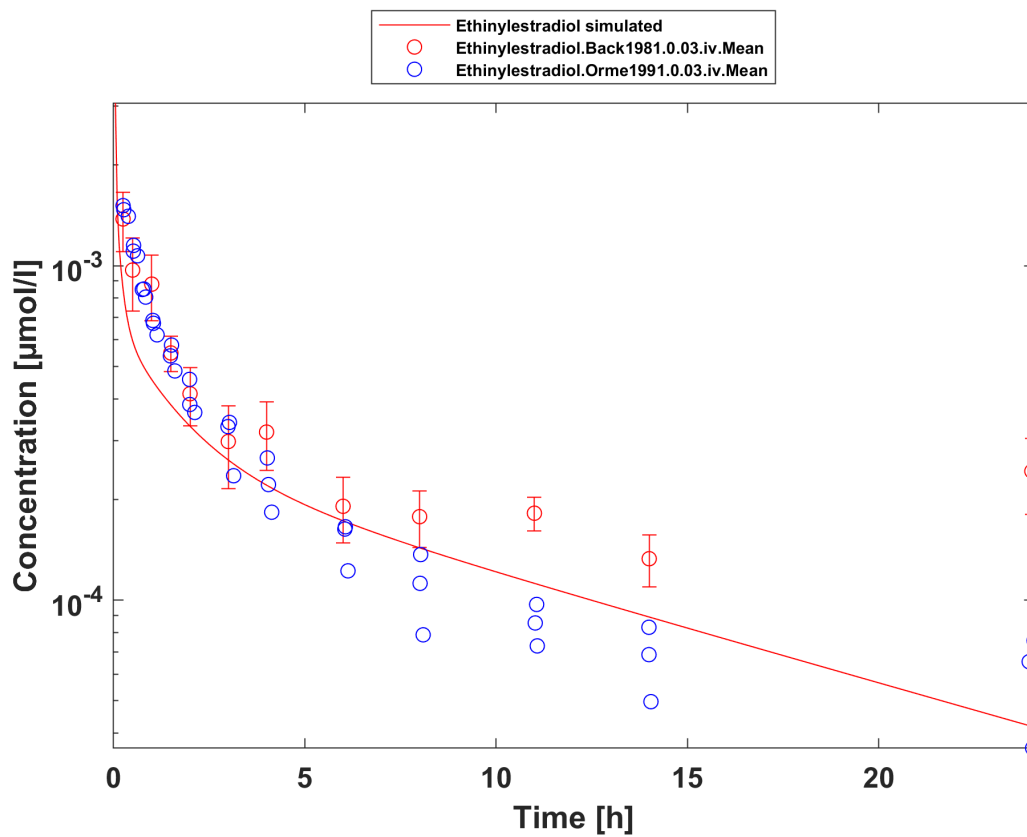
Ethinylestradiol concentration in plasma

GMFE = 1.411117

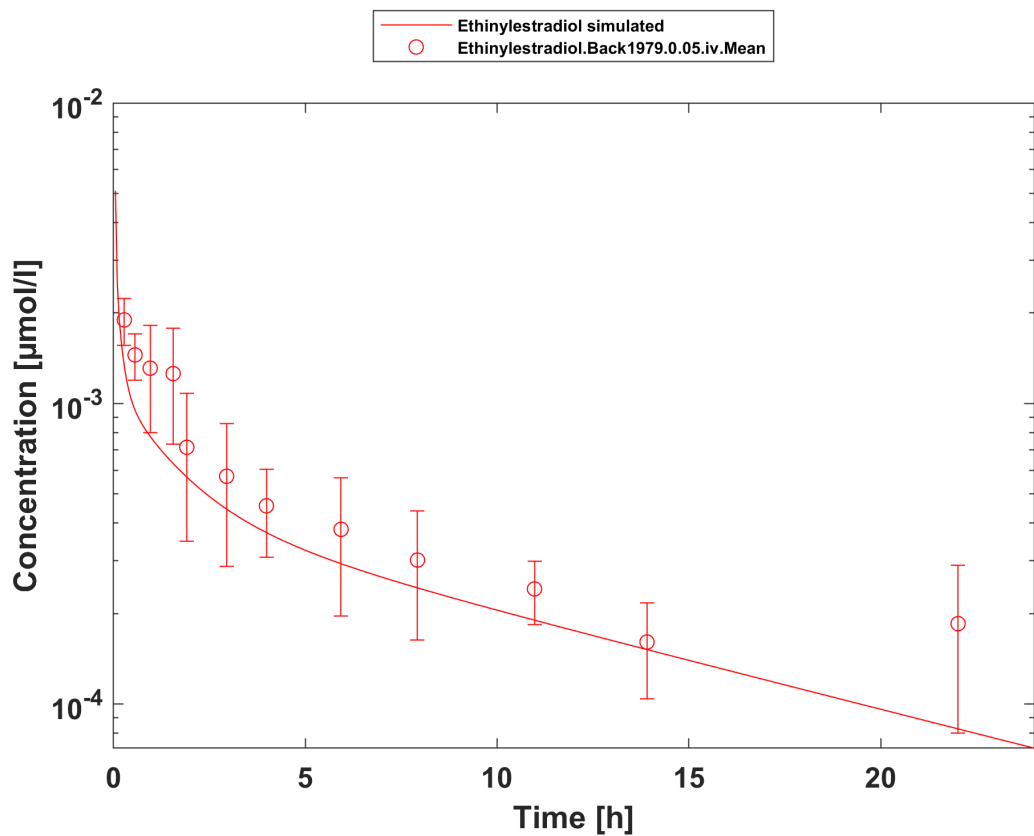
3.3 Concentration-Time Profiles

Simulated versus observed concentration-time profiles of all data listed in [Section 2.2.2](#) are presented below.

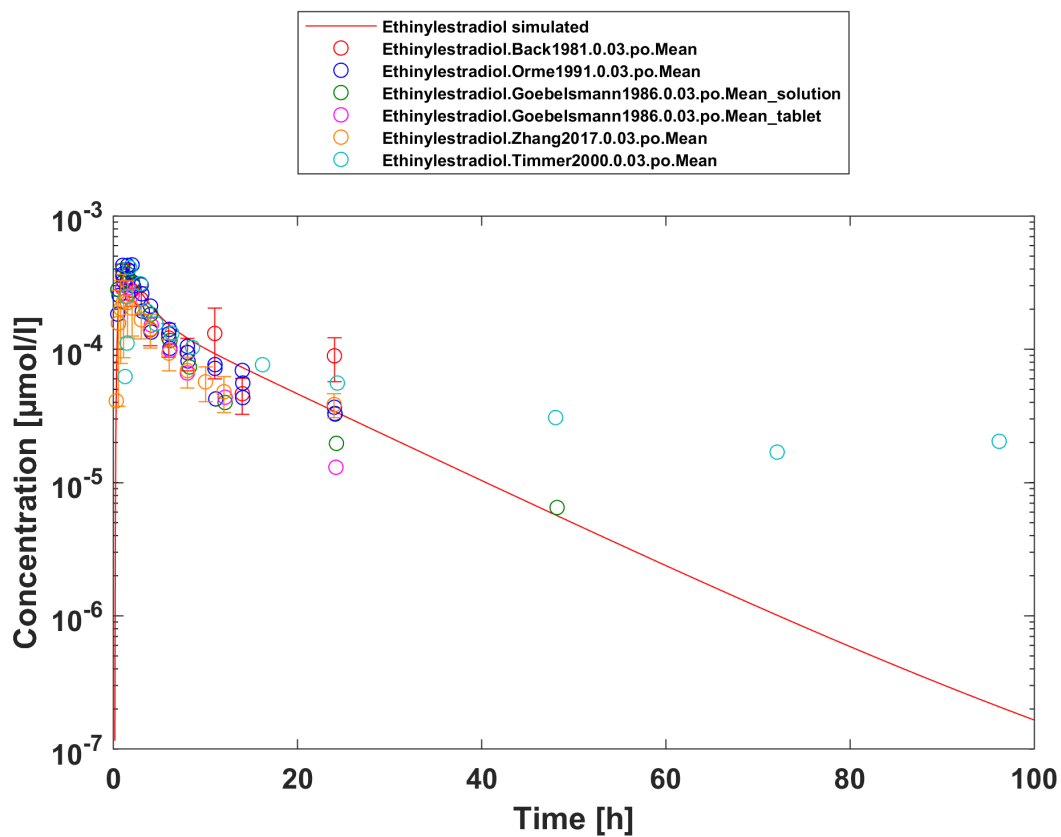
3.3.1 Model Building



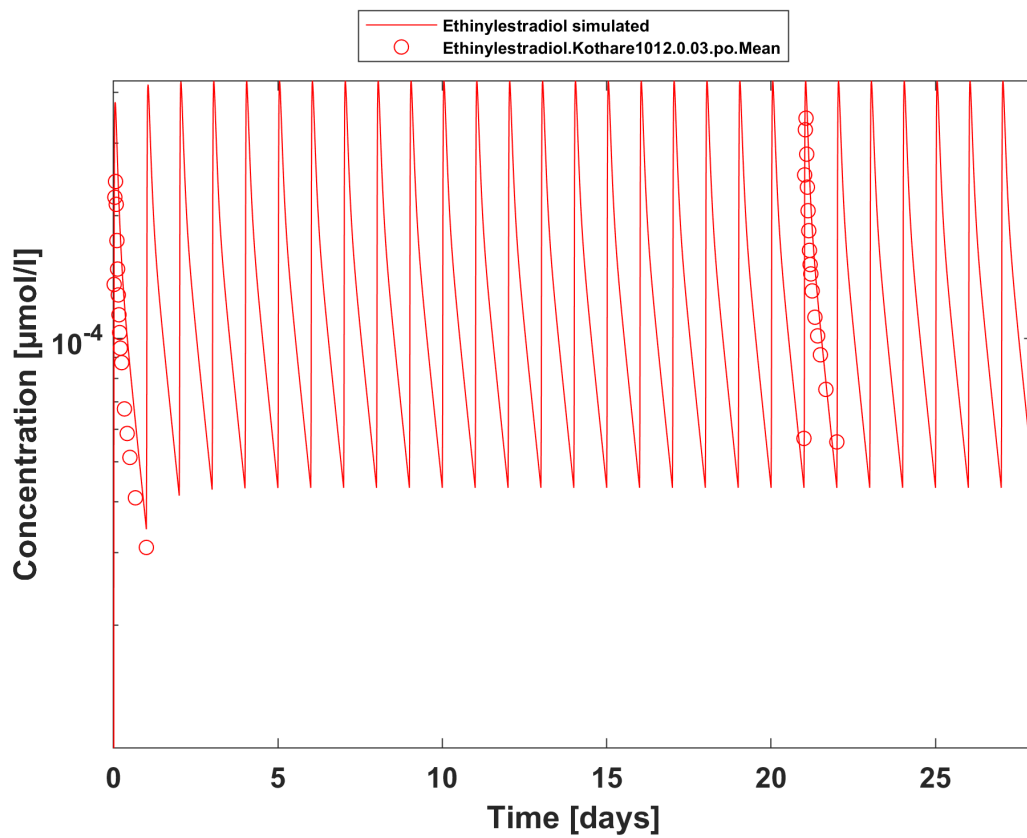
Ethinylestradiol 0.03 mg iv



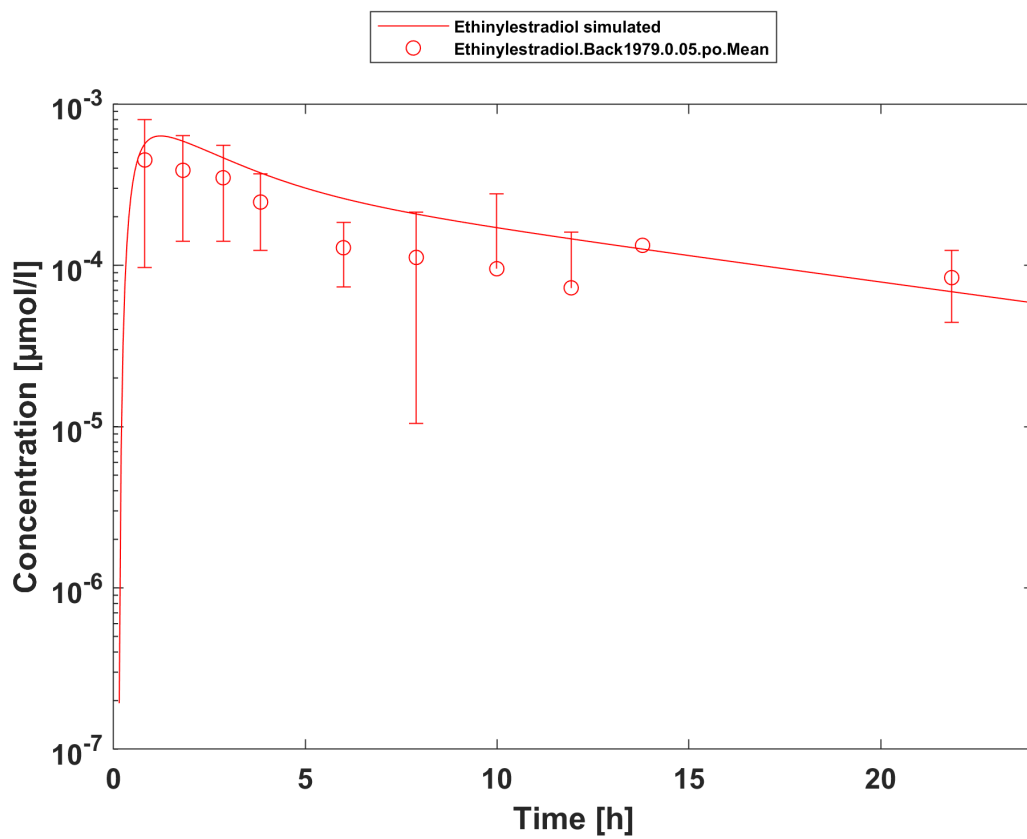
Ethinylestradiol 0.05 mg iv



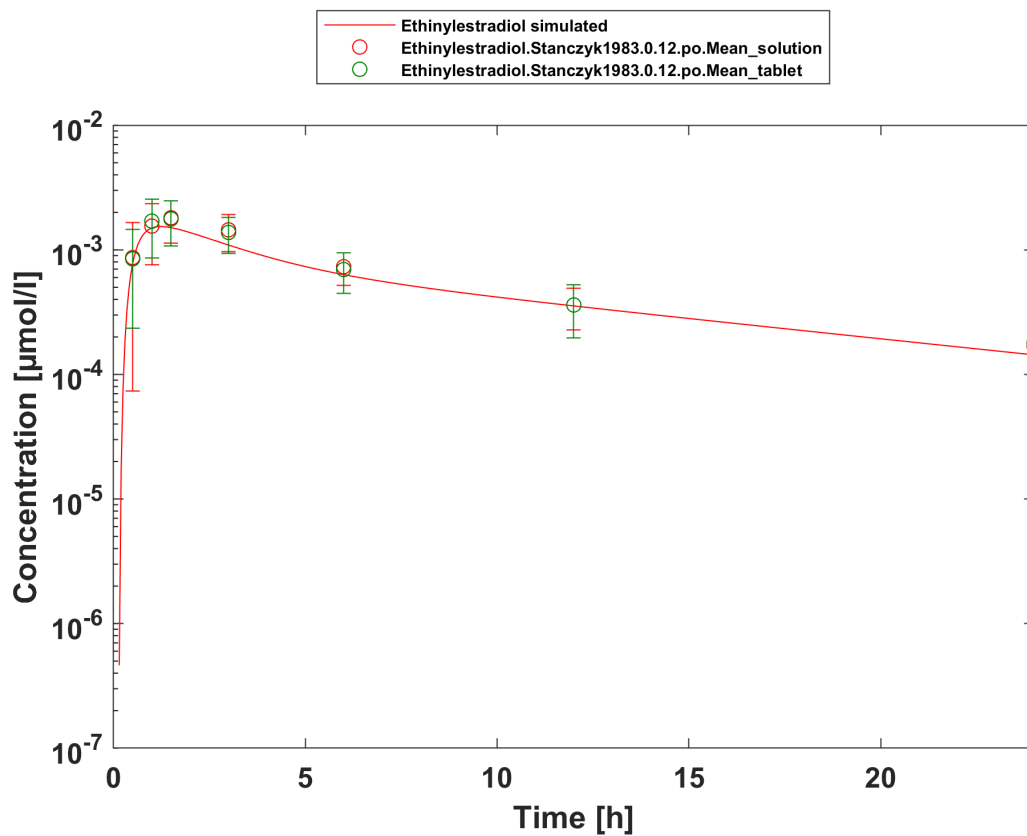
Ethinylestradiol 0.03 mg po



Ethinylestradiol 0.03 mg po 28d

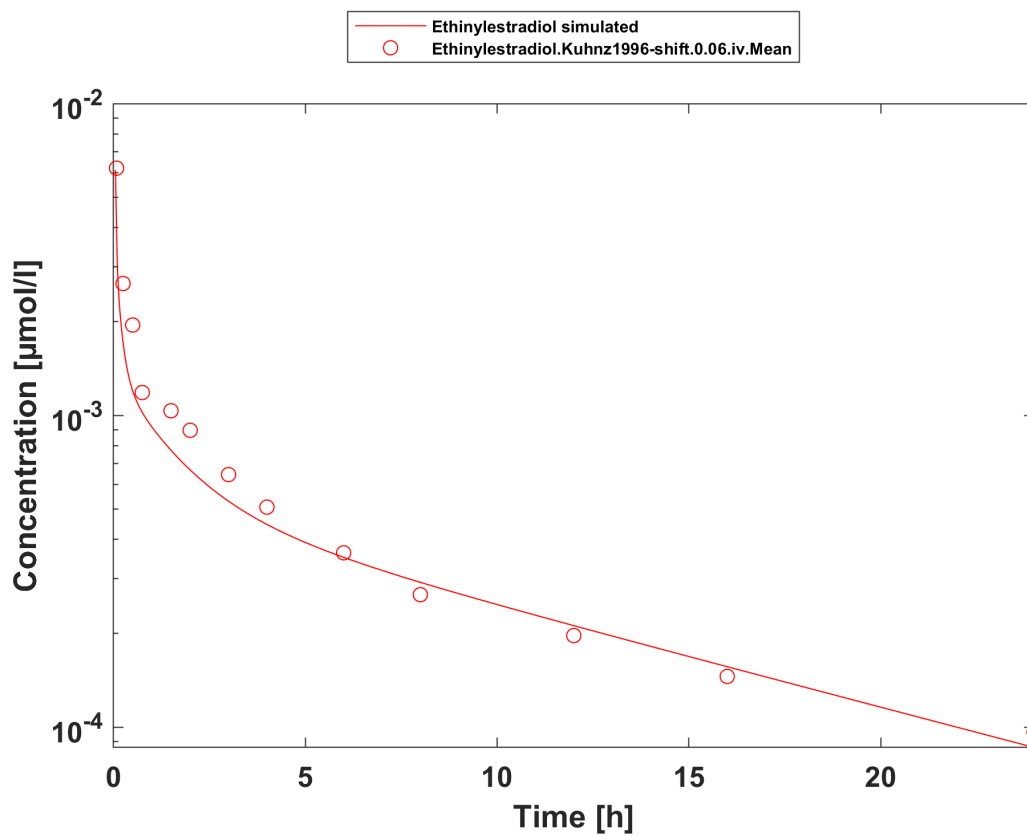


Ethinylestradiol 0.05 mg po

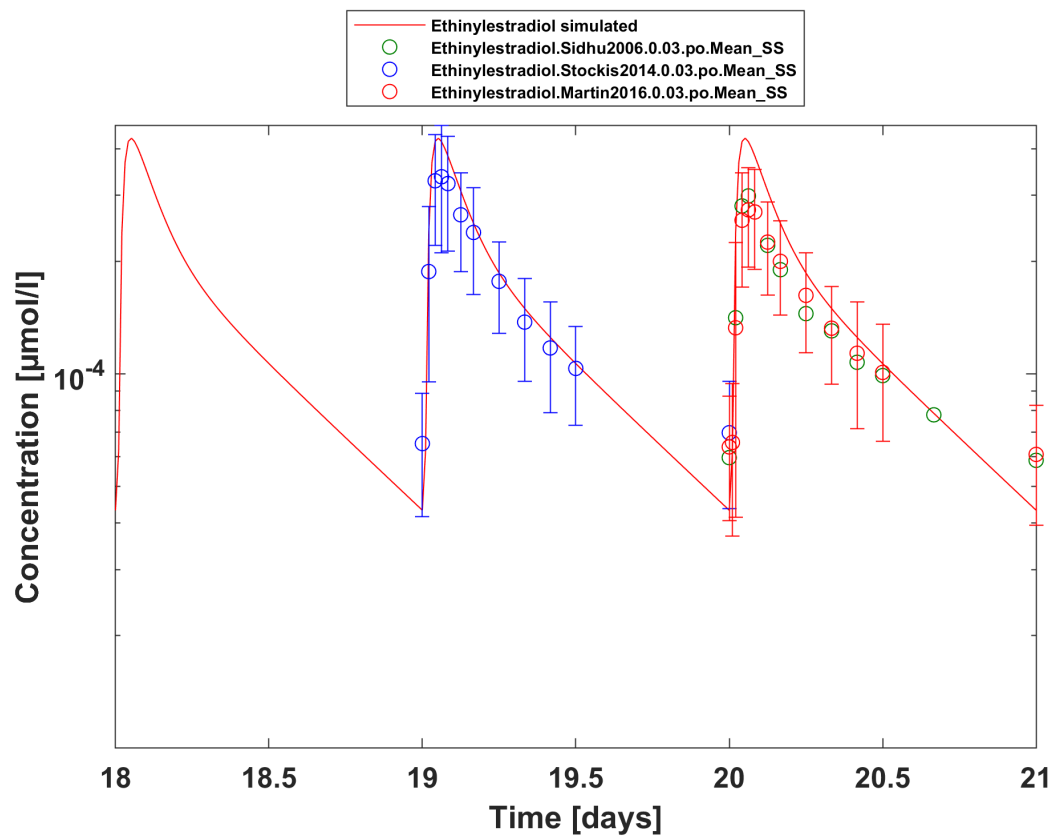


Ethinylestradiol 0.12 mg po

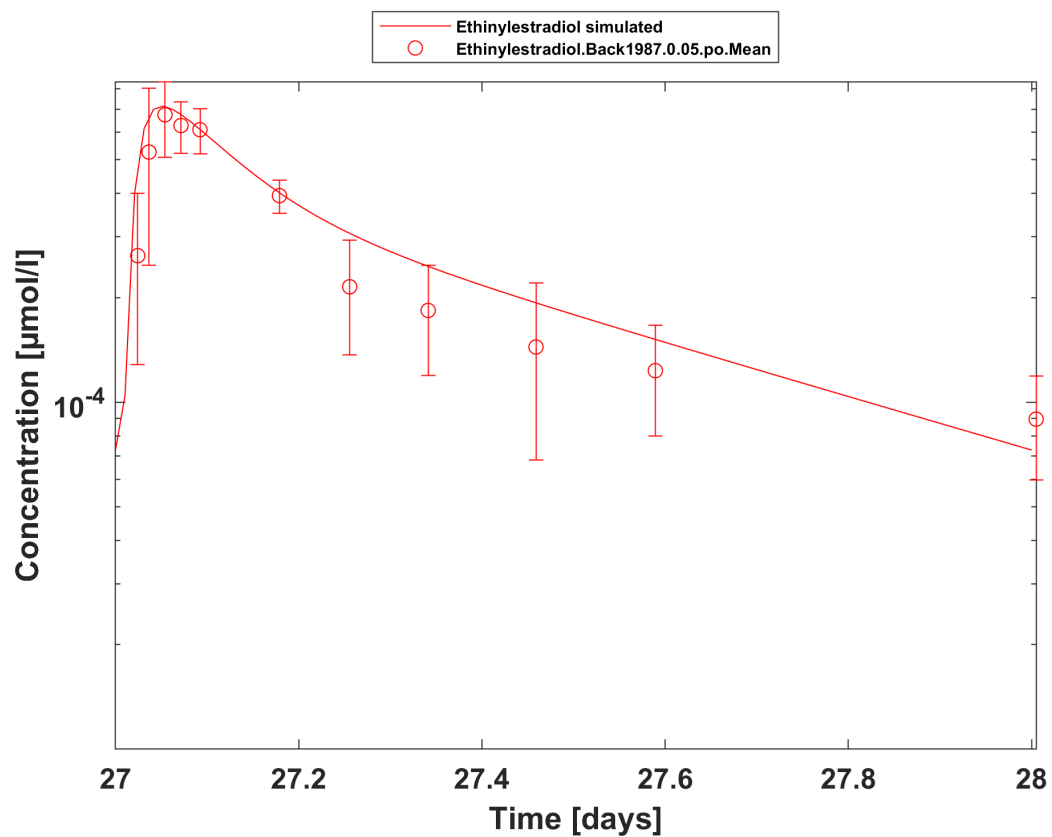
3.3.2 Model Verification



Ethinylestradiol 0.06 mg iv



Ethinylestradiol 0.03 mg po 28d pred



Ethinylestradiol 0.05 mg po 28d

4 Conclusion

The developed PBPK model of ethinylestradiol is able to predict the time-profiles following single and multiple dosing of ethinylestradiol accurately.

The implemented TDI mechanism for ethinylestradiol was not evident in literature ([Zanaflex prescribing information](#), [Karjalainen 2008](#)). The substantial and prolonged inhibition may result from CYP1A2 inhibition by EE-metabolites having a different half-life from the parent. [Chang 2009](#) for example found that the EE-2hydroxy and EE-2methoxy IC50s toward rCYP1A1 and rCYP1A2 are comparable to that of the parent. However, not having the possibility to model EE-metabolites contribution, a time-dependent inhibition function on CYP1A2 was used instead to account for this effect.

5 References

Back 1979 Back DJ, Breckenridge AM, Crawford FE, et al. An investigation of the pharmacokinetics of ethinylestradiol in women using radioimmunoassay. *Contraception*. 1979;20(3):263-273.

Back 1981 Back DJ, Bates M, Breckenridge AM, et al. The pharmacokinetics of levonorgestrel and ethinylestradiol in women - studies with Ovran and Ovranette. *Contraception*. 1981;23(3):229-239.

Back 1987 Back DJ, Grimmer SF, Rogers S, Stevenson PJ, Orme ML. Comparative pharmacokinetics of levonorgestrel and ethinylestradiol following intravenous, oral and vaginal administration. *Contraception*. 1987;36(4):471-479.

Balogh 1995 Balogh A, Boerner A, Kuhn W, Klinger G, Vollandt R, Henschel L. Influence of ethinylestradiol-containing combination oral contraceptives with gestodene or levonorgestrel on caffeine elimination. *Eur J Clin Pharmacol*. 1995;48(2):161-166.

Chang 2009 Chang, S. Y., Chen, C., Yang, Z., Rodrigues, A. D. (2009). Further assessment of 17 α -ethinyl estradiol as an inhibitor of different human cytochrome P450 forms in vitro. *Drug Metabolism and Disposition*, 37(8), 1667-1675.

DrugBank DB00977 (<https://www.drugbank.ca/drugs/DB00977>)

Ezurike 2018 Ezurike U, Humphries H, Dickins M, Neuhoof S, Gardner I, Rowland Yeo K. Risk-Benefit Assessment of Ethinylestradiol Using a Physiologically Based Pharmacokinetic Modeling Approach. *Clin Pharmacol Ther*. 2018;104(6):1229-1239

FDA. QUARTETTE FDA. QUARTETTE (levonorgestrel/ethinyl estradiol and ethinyl estradiol) tablets, for oral use. Website: accessdata.fda.gov/drugsatfda_docs/label/2013/204061s000lbl.pdf. 2013.

Goebelsmann 1986 Goebelsmann U, Hoffman D, Chiang S, Woutersz T. The relative bioavailability of levonorgestrel and ethinyl estradiol administered as a low-dose combination oral contraceptive. *Contraception*. 1986;34(4):341-351.

Granfors 2005 Granfors MT, Backman JT, Laitila J, Neuvonen PJ. Oral contraceptives containing ethinyl estradiol and gestodene markedly increase plasma concentrations and effects of tizanidine by inhibiting cytochrome P450 1A2. *Clin Pharmacol Ther*. 2005;78(4):400-411.

Karjalainen 2008 Karjalainen, M. (Thesis, 2008). Inhibition of CYP1A2-mediated drug metabolism in vitro and in humans: With special emphasis on rofecoxib and other NSAIDs. Website: helda.helsinki.fi/bitstream/handle/10138/23039/inhibiti.pdf?sequence=1&origin=publication_detail

Kothare 2012 Kothare PA, Seger ME, Northrup J, Mace K, Mitchell MI, Linnebjerg H. Effect of exenatide on the pharmacokinetics of a combination oral contraceptive in healthy women: an open-label, randomised, crossover trial. *BMC Clin Pharmacol*. 2012;12:8.

Kuepfer 2016 Kuepfer L, Niederalt C, Wendl T, Schlender JF, Willmann S, Lippert J, Block M, Eissing T, Teutonico D. Applied Concepts in PBPK Modeling: How to Build a PBPK/PD Model. *CPT Pharmacometrics Syst Pharmacol*. 2016 Oct;5(10):516-531.

Kuhn W 1996 Kuhn W, Humpel M, Biere H, Gross D. Influence of repeated oral doses of ethinylestradiol on the metabolic disposition of [¹³C₂]-ethinylestradiol in young women. *Eur J Clin Pharmacol*. 1996;50(3):231-235.

Martin 2016 Martin P, Gillen M, Ritter J, et al. Effects of Fostamatinib on the Pharmacokinetics of Oral Contraceptive, Warfarin, and the Statins Rosuvastatin and Simvastatin: Results From Phase I Clinical Studies. *Drugs R D*. 2016;16(1):93-107.

Orme 1991 Orme M, Back DJ, Ward S, Green S. The pharmacokinetics of ethinylestradiol in the presence and absence of gestodene and desogestrel. *Contraception*. 1991;43(4):305-316.

PK-Sim Ontogeny Database Version 7.3 (<https://github.com/Open-Systems-Pharmacology/OSPSuite.Documentation/blob/38cf71b384cfc25cfa0ce4d2f3addfd32757e13b/PK-Sim%20Ontogeny%20Database%20Version%207.3.pdf>)

Sidhu 2006 Sidhu J, Job S, Singh S, Philipson R. The pharmacokinetic and pharmacodynamic consequences of the co-administration of lamotrigine and a combined oral contraceptive in healthy female subjects. *Br J Clin Pharmacol*. 2006;61(2):191-199.

SmPC Namuscla SmPC Namuscla 167 mg hard capsules, 2019, website [medicines.org.uk/emc/product/9838/smpc](https://www.medicines.org.uk/emc/product/9838/smpc)

Stanczyk 1983 Stanczyk FZ, Mroszczak EJ, Ling T, et al. Plasma levels and pharmacokinetics of norethindrone and ethinylestradiol administered in solution and as tablets to women. *Contraception*. 1983;28(3):241-251..

Stanczyk 2013 Stanczyk FZ, Archer DF, Bhavnani BR. Ethinyl estradiol and 17beta-estradiol in combined oral contraceptives: pharmacokinetics, pharmacodynamics and risk assessment. *Contraception*. 2013;87(6):706-727.

Stockis 2014 Stockis A, Watanabe S, Fauchoux N. Interaction between brivaracetam (100 mg/day) and a combination oral contraceptive: A randomized, double-blind, placebo-controlled study. *Epilepsia*. 2014;55(3):27-31.

Study c13608215-02 Study c13608215. A study to investigate the pharmacokinetic drug-drug interaction following oral administration of ethinylestradiol/levonorgestrel (Microgynon®) and BI 409306 in healthy Korean premenopausal female subjects (an open-label, two-period, fixed-sequence study).” Boehringer Ingelheim Pharma, 06-Aug-2018.

Timmer 2000 Timmer C, Mulders T. Pharmacokinetics of etonogestrel and ethinylestradiol released from a combined vaginal ring. *Clin Pharmacokinet*. 2000;39(3):233-242.

Wang 2004 Wang, B., Sanchez, R.I., Franklin, R.B., Evans, D.C., Huskey, S.E. The involvement of CYP3A4 and CYP2C9 in the metabolism of 17 alpha-ethinylestradiol. *Drug Metab. Dispos*. 32, 1209–1212 (2004).

Wiesinger 2015 Wiesinger, H. et al. Pharmacokinetic interaction between the CYP3A4 inhibitor ketoconazole and the hormone drospirenone in combination with ethinylestradiol or estradiol. *Br. J. Clin. Pharmacol*. 80, 1399–1410 (2015).

Willmann 2007 Willmann S, Höhn K, Edginton A, Sevestre M, Solodenko J, Weiss W, Lippert J, Schmitt W. Development of a physiology-based whole-body population model for assessing the influence of individual variability on the pharmacokinetics of drugs. *J Pharmacokinet Pharmacodyn* 2007, 34(3): 401-431.

Zanaflex prescribing information Zanaflex prescribing information. Website: accessdata.fda.gov/drugsatfda_docs/label/2006/020397s021,021447s002lbl.pdf, 2006, Acorda Therapeutics Inc

Zhang 2017 Zhang C, Li H, Xiong X, et al. An open-label, two-period comparative study on pharmacokinetics and safety of a combined ethinylestradiol/gestodene transdermal contraceptive patch. *Drug Des Devel Ther*. 2017;11:725-731.

6 Glossary

ADME	Absorption, Distribution, Metabolism, Excretion
AUC	Area under the plasma concentration versus time curve
AUCinf	AUC until infinity
AUClast	AUC until last measurable sample
AUCR	Area under the plasma concentration versus time curve Ratio
b.i.d.	Twice daily (bis in diem)
CL	Clearance
Clint	Intrinsic liver clearance
Cmax	Maximum concentration
CmaxR	Maximum concentration Ratio
CYP	Cytochrome P450 oxidase
CYP1A2	Cytochrome P450 1A2 oxidase
CYP2C19	Cytochrome P450 2C19 oxidase
CYP3A4	Cytochrome P450 3A4 oxidase
DDI	Drug-drug interaction
e.c.	Enteric coated
EE	Ethinylestradiol
EM	Extensive metabolizers
fm	Fraction metabolized
FMO	Flavin-containing monooxygenase
fu	Fraction unbound
FDA	Food and Drug administration
GFR	Glomerular filtration rate
HLM	Human liver microsomes
hm	homozygous
ht	heterozygous
IM	Intermediate metabolizers
i.v.	Intravenous
IVIVE	In Vitro to In Vivo Extrapolation
Ka	Absorption rate constant
kcat	Catalyst rate constant
Ki	Inhibitor constant
Kinact	Rate of enzyme inactivation
Km	Michaelis Menten constant
m.d.	Multiple dose
OSP	Open Systems Pharmacology

ADME	Absorption, Distribution, Metabolism, Excretion
PBPK	Physiologically-based pharmacokinetics
PK	Pharmacokinetics
PI	Parameter identification
PM	Poor metabolizers
RT-PCR	Reverse transcription polymerase chain reaction
p.o.	Per os
q.d.	Once daily (quaque diem)
SD	Single Dose
SE	Standard error
s.d.SPC	Single doseSummary of Product Characteristics
SD	Standard deviation
TDI	Time dependent inhibition
t.i.d	Three times a day (ter in die)
UGT	Uridine 5'-diphospho-glucuronosyltransferase
UM	Ultra-rapid metabolizers